

Linear Layer Thermal Analysis of Lithium-Ion Battery Cooling System for Electric Vehicles

^[1]Dr. Ashok Kumar Vootla, ^[2]Lakka Naveen

Associate professor, Dept. Mechanical engineering mother Theresa College of engg & tech.
Peddapalli, , india

Mechanical engineering , mother Theresa College of engg & tech. Peddapalli, , india

E-Mail: ashoko.vootla9@gmail.com , naveenlakka91@gmail.com

Abstract:

Lithium-ion power battery has become one of the main power sources for electric vehicles and hybrid electric vehicles because of superior performance compared with other power sources. In order to ensure the safety and improve the performance, the maximum operating temperature and local temperature difference of batteries must be maintained in an appropriate range. In this thesis we are experimenting the cooling system of the Li-ion batteries combined with a phase change material and heat pipes to control abnormal heat emissions to improve the battery performance and efficiency. The hybrid cooling system solid model is prepared in CREO software and the CFD analysis is evaluated in the ANSYS software. The hybrid cooling system model designed with different types of heat pipe designs and is analyzed with different mass flow rates (30& 50L/min). The comparison is done among three kinds of the hybrid cooling system (combining the heat pipes and PCM) with numerical analysis of the heat balance and thermal analysis. In this thesis the pressure, velocity, heat transfer coefficient, mass flow rate and heat transfer rate for the different designs of heat pipe and different mass flow inlets is determined in CFD analysis. Two types of phase change materials (RT50 & Li Fe PO₄) are used to determine the temperature distribution and heat flux. The results of the analysis compare the heat transfer rate of the four different kinds of the cooling system design.

Keywords: Battery thermal management, Li-ion battery, Phase-change material, Heat pipe.

I. INTRODUCTION

Hybrid Electric Vehicles (HEVs) are the first steps to make the transition possible to the fully electrification of the automotive sector in the future. In principle, there are two energy sources in HEVs: the conventional internal combustion engine (ICE),

which uses mainly gasoline or diesel operates in combination with an electric motor generally powered by battery or a combination of battery and electrical double-layer capacitors (EDLCs). The HEVs have the advantage of reducing the fuel consumption and emissions. The electric motor allows energy recovery to the battery system during braking, provides additional power to assist the ICE during pick power demand, and then allows reducing the size and power of the ICE.

Lithium-ion battery (LIB) has received considerable attention for traction uses due to the higher energy density (70-170 Wh/kg), power capabilities, lowest standard reduction voltage ($E_0 = -3.04V$) and low atomic mass compared to previous battery technologies. The required amount of energy stored in PHEVs and EVs is much higher than for HEVs in order to be able to travel long distances in all electric range. The basic working principle of the LIB is, during charging lithium-ions are extracted from the cathode and migrate via the electrolyte into the anode. The reverse mechanism occurs during discharging.

II. LITERATURE REVIEW

Ahmadou Samba [1] presents a brief description of the environmental impact of the transportation sector regarding energy consumption and gas emissions. In addition, the state-of-the-art of EVs, HEVs and PHEVs is presented as potential solution of the environmental issues. Furthermore, the characteristics and specifications of the different batteries used in these vehicles are compared and analyzed. Finally, the specifications of some recent commercial vehicles are also reported.

Mohammad Rezwana Khan [2] studied the prevailing standards and scientific literature offer a wide range of options for the construction of a battery thermal management system (BTMS). The design of an innovative yet well-functioning BTMS requires strict

supervision, quality audit and continuous improvement of the whole process. It must address all the current quality and safety (Q&S) standards. In his review article, an effective battery thermal management is sought considering the existing battery Q&S standards and scientific literature. The article contains a broad overview of the current existing standards and literature on a generic compliant BTMS. Additionally, the article delivers a set of recommendations to make an effective BTMS.

Bahman Shabani and Manu Biju [3] the main challenge associated with renewable energy generation is the intermittency of the renewable source of power. Because of this, back-up generation sources fuelled by fossil fuels are required. In stationary applications whether it is a back-up diesel generator or connection to the grid, these systems are yet to be truly emissions-free. One solution to the problem is the utilization of electrochemical energy storage systems (ESS) to store the excess renewable energy and then reusing this energy when the renewable energy source is insufficient to meet the demand.

Zhoujian An [4] Lithium-ion power battery has become one of the main power sources for electric vehicles and hybrid electric vehicles because of superior performance compared with other power sources. In order to ensure the safety and improve the performance, the maximum operating temperature and local temperature difference of batteries must be maintained in an appropriate range. The effect of temperature on the capacity fade and aging are simply investigated. The electrode structure, including electrode thickness, particle size and porosity, are analyzed. It is found that all of them have significant influences on the heat generation of battery.

III. MODELLING AND ANALYSIS

Generally, soft pouch cells for BEVs and PHEVs have small thicknesses, which vary between 5 and 20 mm, depending on the battery cell capacity. The used LiFePO_4 /graphite lithium-ion pouch cell with the size of the different domains (Tabs, case and electrode domains) is illustrated. These domains are made of different materials.

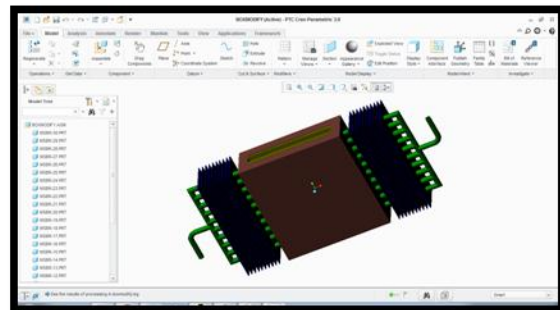
The pouch cell cooled by two cold plates with the same designs and dimensions. The cold plates are located on both sides of the pouch cell. The heat is generated by the battery, transferred into the cold plates, and removed throughout the cooling channels. Three cold plates designs are investigated at various

discharge current rates (2 It, 4 It and 6 It) in order to illustrate the most efficient in terms of the maximum temperature rising and temperature distribution of the battery cell.

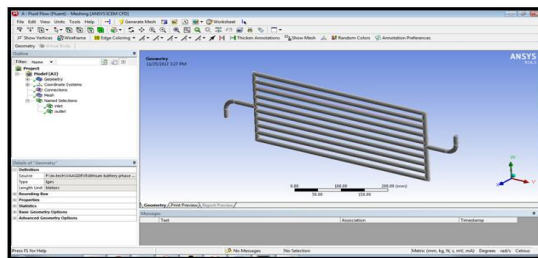
The whole system is insulated in order to quantify the effectiveness's of the different cold plate designs and to represent the real situation in pack level where the battery are covered by protective material. The cooling plates and cooling channel are made of aluminum and copper, respectively.

The solid model of the combined cooling system is prepared in the CREO parametric and the thermal analysis, CFD analysis is carried out in the ANSYS software. The combined cooling system is combined with the liquid cooling and phase change material cooling and the three different kinds of heat pipes are considered with two mass flow rates 30 & 50 L/min. the phase change materials that are considered are RT50 & LiFePO_4 .

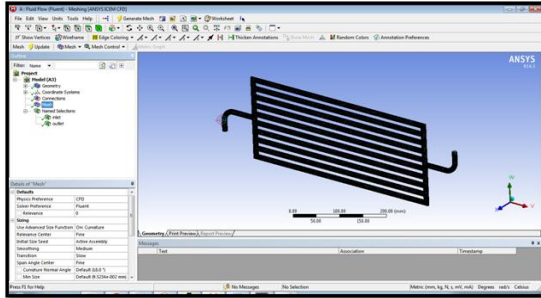
The three different kinds of the cooling model designed in the CREO parametric are battery covered with PCM and straight type heat pipes, box type heat pipes and bent type heat pipes. With the CFD analysis performed on these three models the box type heat pipes are selected for the further thermal analysis of the cooling system models with two different kinds of phase change materials because comparatively the heat transfer is more.



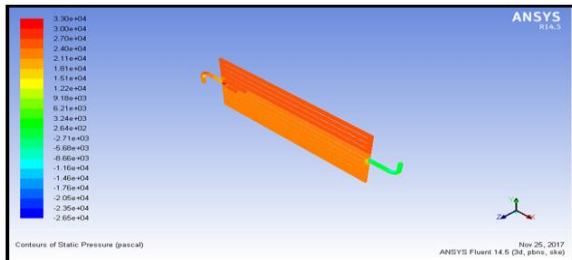
**MASS FLOW INLET - 30L/min
IMPORTED MODEL**



MESHED MODEL

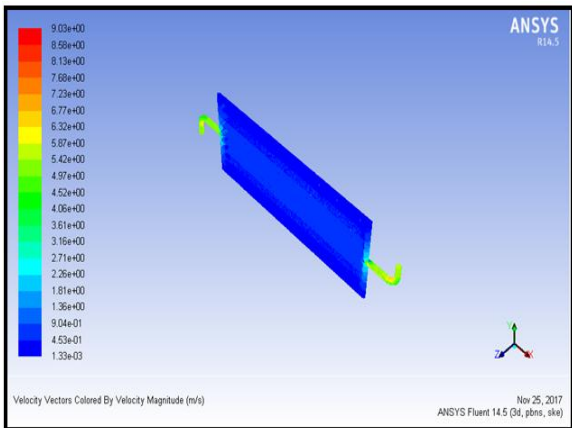


PRESSURE



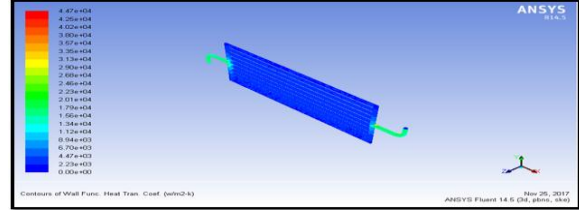
According to the above contour plot, the maximum static pressure inlet of the heat pipes at one end of the tubes because the applying the boundary conditions at inlet of the heat pipes and minimum static pressure at the fluid outlet. According to the above contour plot, the maximum pressure is 3.30×10^4 and minimum static pressure is -2.65×10^4 .

VELOCITY



According to the above contour plot, the maximum velocity magnitude of the inside the heat pipes, because the applying the boundary conditions at inlet of the heat pipes and minimum velocity magnitude at upper surface of the heat pipes. According to the above contour plot, the maximum velocity is 9.03×10^0 and minimum velocity is 1.33×10^{-3} .

HEAT TRANSFER COEFFICIENT



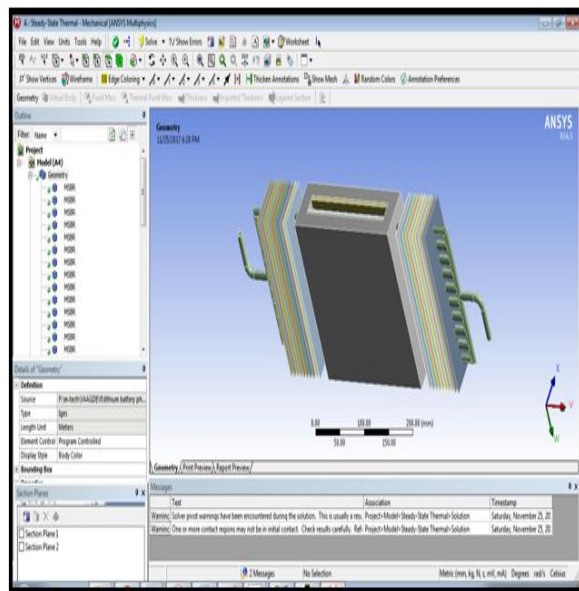
According to the above contour plot, the maximum heat transfer coefficient of the heat pipes at one end of the heat pipe and minimum heat transfer coefficient another end of the heat pipe. According to the above contour plot, the maximum heat transfer coefficient is $4.47 \times 10^4 \text{ w/m}^2\text{-k}$ and minimum heat transfer coefficient is $2.23 \times 10^3 \text{ w/m}^2\text{-k}$.

MASS FLOW RATE & HEAT TRANSFER RATE

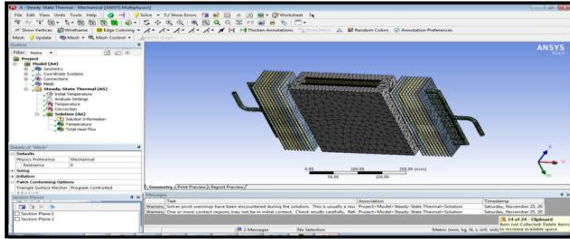
Mass Flow Rate		(kg/s)
inlet		0.51000005
interior-msbr		-0.077392489
outlet		-0.51741242
wall-msbr		0
Net		-0.007412374
Total Heat Transfer Rate		(w)
inlet		116985.2
outlet		-118685.27
wall-msbr		0
Net		-1700.0625

MATERIAL- RT50 (PHASE CHANGE MATERIAL)

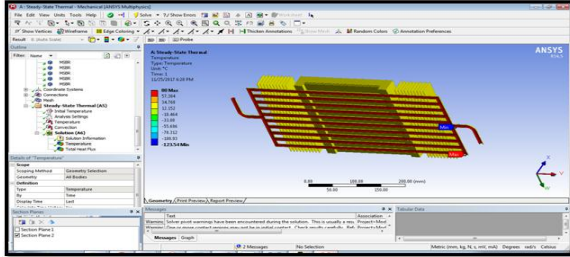
Imported model



Meshed model

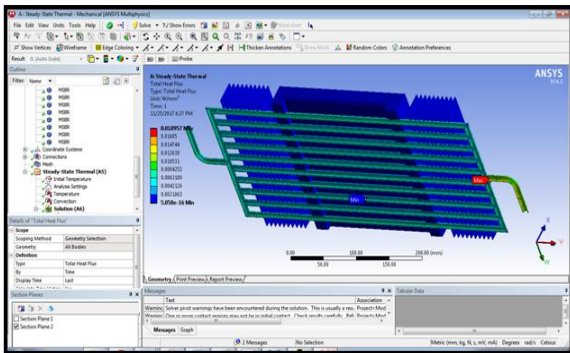


Temperature



According to the contour plot, the temperature distribution maximum temperature at inside of the heat pipe because the fluid passing through inside of the heat pipe. So we are applying the temperature inside of the heat pipe and applying the convection except inside the heat pipe. Then the maximum temperature at tubes and minimum temperature at cooling fins.

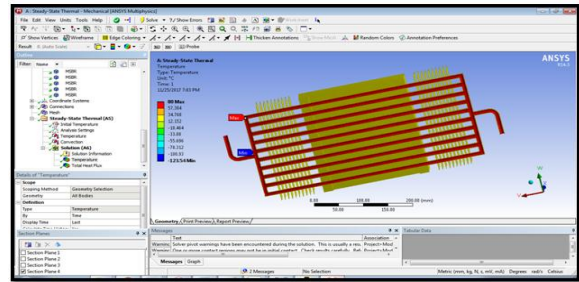
Heat flux



According to the contour plot, the maximum heat flux at inside the heat pipes because the fluid passing through inside of the heat pipe. So we are applying the temperature inside of the heat pipe and applying the convection except inside the heat pipe. Then the maximum heat flux at inside the heat pipe and minimum heat flux at cooling fins. According to the above contour plot, the maximum heat flux is 0.018957w/mm² and minimum heat flux is 5.058e-16w/mm².

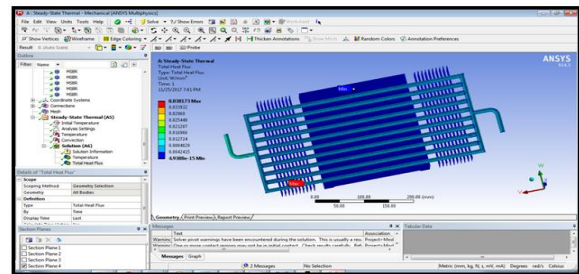
MATERIAL- Li Fe PO4 (PHASE CHANGE MATERIAL)

Temperature



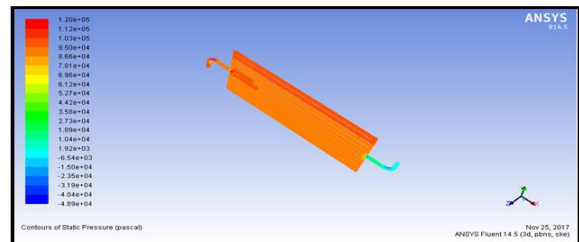
According to the contour plot, the temperature distribution maximum temperature at inside of the heat pipe because the fluid passing through inside of the heat pipe. So we are applying the temperature inside of the heat pipe and applying the convection except inside the heat pipe. Then the maximum temperature at tubes and minimum temperature at cooling fins.

Heat flux



According to the contour plot, the maximum heat flux at inside the heat pipes because the fluid passing through inside of the heat pipe. So we are applying the temperature inside of the heat pipe and applying the convection except inside the heat pipe. Then the maximum heat flux at inside the heat pipe and minimum heat flux at cooling fins. According to the above contour plot, the maximum heat flux is 0.038173w/mm² and minimum heat flux is 4.9388e-15w/mm².

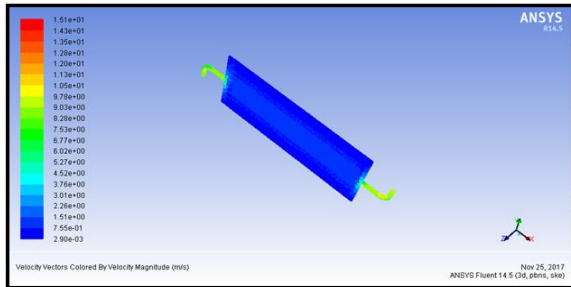
MASS FLOW INLET - 50L/min PRESSURE



According to the above contour plot, the maximum static pressure inlet of the heat pipes at one end of the tubes because the applying the boundary conditions at inlet of the heat pipes and minimum static pressure at the fluid outlet. According to the above

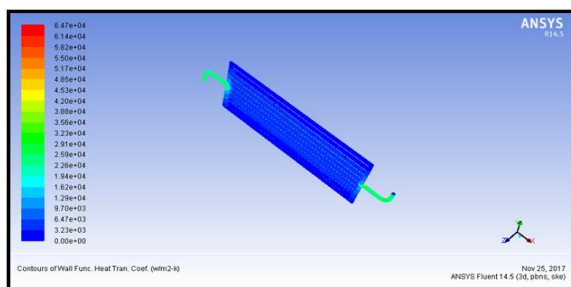
contour plot, the maximum pressure is 1.20×10^5 and minimum static pressure is -4.89×10^4 .

VELOCITY



According to the above contour plot, the maximum velocity magnitude of the inside the heat pipes, because the applying the boundary conditions at inlet of the heat pipes and minimum velocity magnitude at upper surface of the heat pipes. According to the above contour plot, the maximum velocity is 1.51×10^1 and minimum velocity is 2.90×10^{-3} .

HEAT TRANSFER COEFFICIENT



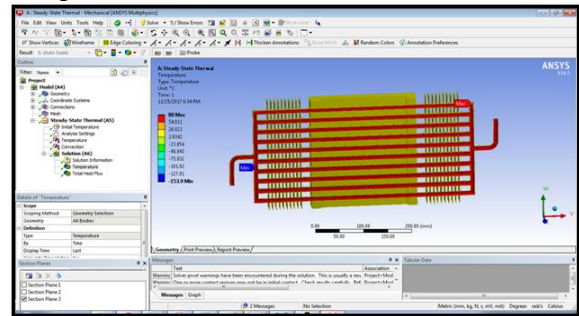
According to the above contour plot, the maximum heat transfer coefficient of the heat pipes at one end of the heat pipe and minimum heat transfer coefficient another end of the heat pipe. According to the above contour plot, the maximum heat transfer coefficient $6.47 \times 10^4 \text{ W/m}^2\text{-k}$ and minimum heat transfer coefficient is $3.23 \times 10^3 \text{ W/m}^2\text{-k}$.

MASS FLOW RATE & HEAT TRANSFER RATE

Mass Flow Rate		(kg/s)
inlet	msbr	0.8500002
interior	msbr	-0.1591023
outlet	msbr	-0.86004871
wall	msbr	0
Net		-0.010048509
Total Heat Transfer Rate		(w)
inlet	msbr	194975.33
outlet	msbr	-197280.11
wall	msbr	0
Net		-2304.7813

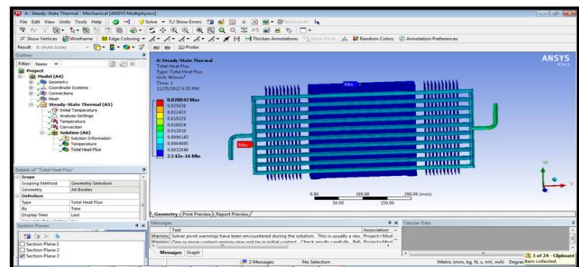
MATERIAL- RT50 (PHASE CHANGE MATERIAL)

Temperature



According to the contour plot, the temperature distribution maximum temperature at inside of the heat pipe because the fluid passing through inside of the heat pipe. So we are applying the temperature inside of the heat pipe and applying the convection except inside the heat pipe. Then the maximum temperature at tubes and minimum temperature at cooling fins.

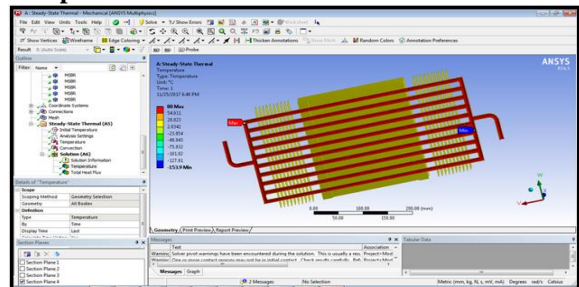
Heat flux



According to the contour plot, the maximum heat flux at inside the heat pipes because the fluid passing through inside of the heat pipe. So we are applying the temperature inside of the heat pipe and applying the convection except inside the heat pipe. Then the maximum heat flux at inside the heat pipe and minimum heat flux at cooling fins. According to the above contour plot, the maximum heat flux is 0.028843 W/mm^2 and minimum heat flux is $2.142 \times 10^{-16} \text{ W/mm}^2$.

MATERIAL- Li Fe PO4 (PHASE CHANGE MATERIAL)

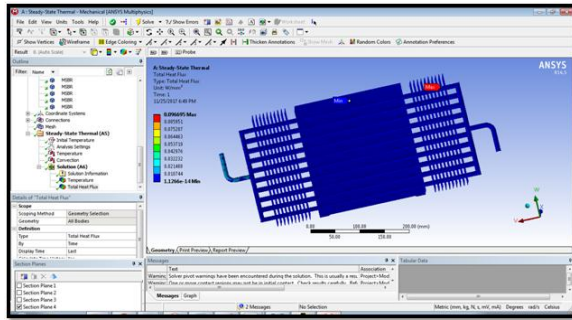
Temperature



According to the contour plot, the temperature

distribution maximum temperature at inside of the heat pipe because the fluid passing through inside of the heat pipe. So we are applying the temperature inside of the heat pipe and applying the convection except inside the heat pipe. Then the maximum temperature at tubes and minimum temperature at cooling fins.

Heat flux



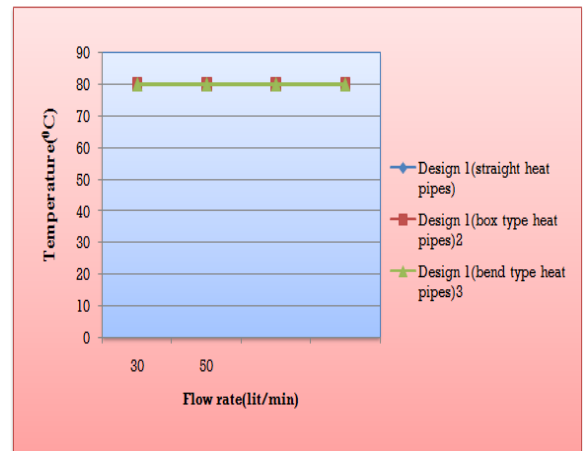
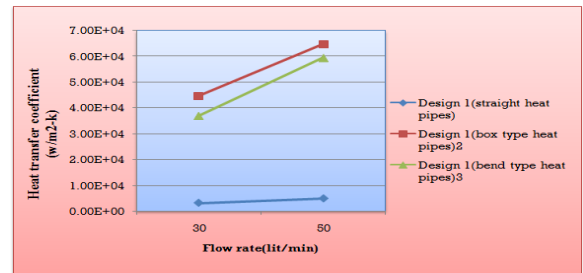
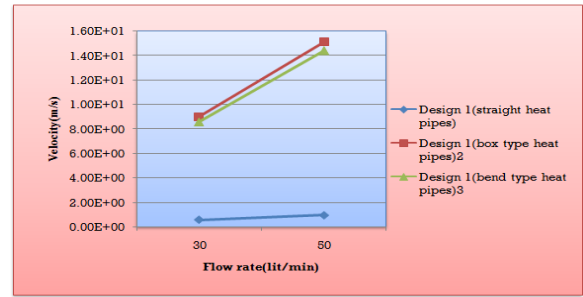
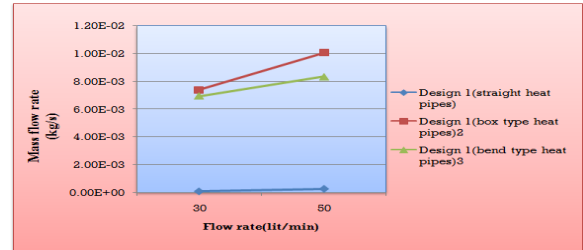
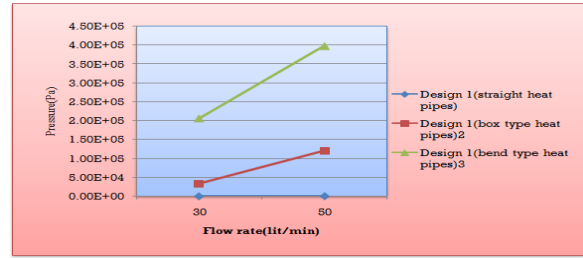
According to the contour plot, the maximum heat flux at inside the heat pipes because the fluid passing through inside of the heat pipe. So we are applying the temperature inside of the heat pipe and applying the convection except inside the heat pipe. Then the maximum heat flux at inside the heat pipe and minimum heat flux at cooling fins.

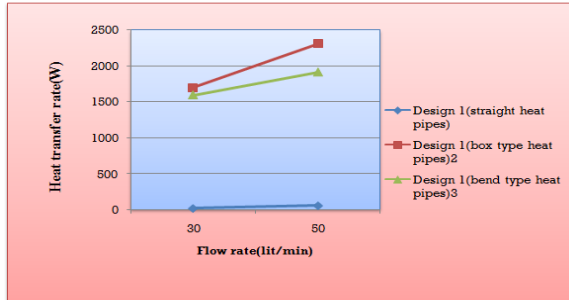
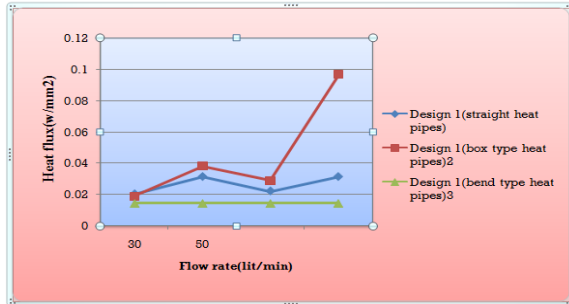
IV. RESULTS

Models	Flow rate (lit/min)	Pressure (Pa)	Velocity (m/s)	Heat transfer coefficient (w/m ² -k)	Mass flow rate (kg/s)	Heat transfer rate (W)
Design1 (straight heat pipes)	30	2.47e+02	5.77e-01	3.23e+03	8.1002e-05	18.507813
	50	5.92e+02	9.57e-01	4.92e+03	0.0002552	58.59375
Design 2(box type heat pipes)	30	3.30e+04	9.03e+00	4.47e+04	0.0074	1700.0625
	50	1.20e+05	1.51e+01	6.47e+04	0.010048	2304.7813
Design 3(bend type heat pipes)	30	2.06e+05	8.58e+00	3.70e+04	0.0069425	1592.7266
	50	3.98e+05	1.44e+01	5.95e+04	0.008344	1913.5

Models	Flow rate (lit/min)	Material	Temperature(°C)	Heat flux(w/mm ²)
Design1 (straight heat pipes)	30	PCMRT50	80	0.020264
		PCMLi Fe PO4	80	0.031486
	50	PCMRT50	80	0.022175
		PCMLi Fe PO4	80	0.0315
Design 2(box type heat pipes)	30	PCMRT50	80	0.018957
		PCMLi Fe PO4	80	0.038173
		80		
	50	PCMRT50	80	0.028843
		PCMLi Fe PO4	80	0.096695
		80		
Design 3(bend type heat pipes)	30	PCMRT50	80	0.014355
		PCMLi Fe PO4	80	0.014391
		80		
	50	PCMRT50	80	0.014376
		PCMLi Fe PO4	80	0.014393
		80		

GRAPHS





V. CONCLUSION

Lithium-ion power battery has become one of the main power sources for electric vehicles and hybrid electric vehicles because of superior performance compared with other power sources. In order to ensure the safety and improve the performance, the maximum operating temperature and local temperature difference of batteries must be maintained in an appropriate range. In thesis the modeling in CREO parametric software and analysis done in ANSYS. The model designed with different type of heat pipe shapes and analyzes the heat pipe with different mass flow inlets (30& 50L/min).

By observing the CFD analysis mass flow rate, heat transfer rate, heat transfer coefficient values are increased by increasing the mass flow inlets and heat transfer rate more at design2 (box type heat pipes).

By observing the thermal analysis the heat flux value is more for lithium ion phosphate phase change material than RT50 phase change material at design2 (box type heat pipes)

So it can be concluded the design2 (box type heat pipes) is better model for Lithium-ion power battery cooling system.

REFERENCES

1. Wagner, R. Valve regulated lead-acid batteries for telecommunications and UPS applications. In Valve-Regulated Lead-Acid Batteries; Rand, D.J., Ed.; Elsevier B.V.: Oxford, UK, 2004; pp. 435–465.

2. Percy, K. Ausnet Testing New Battery System to Curb Power Outages in Summer. Available online: <http://www.abc.net.au/news/2015-01-07/ausnet-trialling-new-system-to-curb-power-outages-on-hot-days/6004454> (accessed on 30 May 2015). *Energies* 2015, 8 10172

3. Pesaran, A.A. Battery thermal models for hybrid vehicle simulations. *J. Power Sci.* 2002, 110, 377–382.

4. Rothgang, S.; Rogge, M.; Becker, J.; Sauer, D.U. Battery design for successful electrification in public transport. *Energies* 2015, 8, 6715–6737.

5. Shabani, B.; Andrews, J. Standalone solar-hydrogen systems powering fire contingency networks. *Int. J. Hydrogen Energy* 2015, 40, 5509–5517.

6. Pesaran, A.; Vlahinos, A.; Stuart, T. Cooling and Preheating of Batteries in Hybrid Electric Vehicles; National Renewable Energy Laboratory (NREL): Colorado, CO, USA, 2003.

7. Ji, Y.; Wang, Y. Heating strategies for Li-ion batteries operated from subzero temperatures. *Electrochim. Acta* 2013, 107, 664–674.

8. Szent-Varga, D.; Horvath, G.; Rencz, M. Thermal characterization and modelling of lithium-based batteries at low ambient temperature. In Proceedings of the 14th International Workshop on Thermal Investigation of ICs and Systems, 2008 (THERMINIC 2008), Rome, Italy, 24–26 September 2008.